CHAPTER XXVI-1

THE UPPER LIMB BONES OF THE SPY NEANDERTALS

Anne HAMBÜCKEN

Abstract

The upper limb bones (humeri, radii and ulnae) of two adult Neandertals, Spy I and II, were discovered at the Spy site. Their re-examination led to identify the Spy 7A ulna as Neolithic and to exclude it from the Spy I upper limb. A novel attribution of the radii is also suggested, both Spy 6 and Spy 15B possibly belonging to Spy II.

This new study confirms that Spy I and Spy II are globally well-integrated within the variability of the "classic" Neandertals. The marked size difference between their upper limb bones supports the hypothesis of a sexual dimorphism, with Spy II most likely being a male, and Spy I possibly a female. Their most distinctive common feature, when compared to other Neandertals, is the morphology of the deltoid tuberosity of their humeri. This muscle insertion appears as very narrow, curved, and laterally swerved, with a well-developed and elongated anterior crest. If both Spy 6 and Spy 15B radii indeed belong to Spy II, this individual displays an unusually high interosseus border asymmetry and shows very lateralised humeral deltoid tuberosities. The level of humeral shaft asymmetry of Spy II appears otherwise close to that of the Neandertal males, while the asymmetry of Spy I is similar to that of the Tabun C1 female. The greater asymmetry observed in Spy II further indicates more lateralised and specialised activities than in Spy I.

At the functional level, the general morphology of the Spy upper limb suggests a reduced abduction strength but powerful flexion/extension and rotation movements of the shoulder, as well as stronger and ampler flexion and pronosupination of the elbow as compared to modern humans.

MATERIAL AND METHOD

The Spy site has delivered remains of the upper limb skeleton of two adult Neandertals. These bones were compared to the following Neandertal (N) original fossils: Neandertal 1 (Germany); Krapina, humeri 159 to 166, 169 to 174, 176 and 178; radii 189 and 190; ulnae 189 to 195, 188-5, and 188-8 (Croatia); Lezetxiki 1 and Vilafamès CTF1 (Spain); La Chapelle-aux-Saints 1, Combe-Grenal 567, La Ferrassie 1 and 2, Hortus 21 and 22, Macassargues 2, La Quina 5, Regourdou 1 and Saint-Césaire 1 (France); Shanidar 4, 5, 6 and 8 (Iraq); Amud 1, Kebara 2 and Tabun C1 (Israel).

Several modern human (MH) collections of various temporal and geographical origins (ST1) served as comparison sample. The measurements and indices used in this study are listed and described in Tables 2 to 5 and illustrated in SF1. Results are presented as means ± standard errors. The Neandertal and modern human means were compared with the Student's t-test and are considered as significantly different when $p \leq 0.05$. The Neolithic bones found at Spy, as well as Mosan Neolithics from the La Cave cavern in Maurenne (RBINS, Belgium), were added to the study to examine the taxonomic attribution of the 7A ulna and the 336a and 181a radii (see below). The methodology used to process the cross-sections is described in chapter XXII (Balzeau *et al.*, this volume).

DESCRIPTION

State of preservation and bone attribution

The upper limb bones traditionally attributed to the Spy Neandertals consist of four humeri, two radii and three ulnae. The fossils are in good shape, although only partially preserved. There is no deformation and no obvious sign of pathology.

The Spy 5A right humerus has been reconstituted from two pieces. It comprises the shaft, starting from about the deltoid tuberosity mid-length, and the distal extremity of the bone. The medial epicondyle is missing, there is some damage to the medial part of the trochlea, and a shard of the humeral pallet area, located above the coronoid fossa, is missing.

The Spy 5B left humerus is composed of two pieces constituting most of the shaft, from the surgical neck to the beginning of the humeral pallet widening.

The Spy 14A left humerus has been reconstructed from three fragments. The shaft is intact starting from the distal part of the greater tubercle ridge. The distal extremity is well-preserved, except for some damage to the medial part of the trochlea, to the posterior side of the medial epicondyle, and for a missing shard on the border of the medial pillar.

The Spy 14B right humerus is pieced together from two fragments. The shaft is preserved from the distal part of the greater tubercle ridge to the distal extremity. The lateral epicondyle and the part of the bone situated behind the capitulum are missing on an otherwise well-preserved distal epiphysis.

The Spy 6 left radius is reconstructed from three pieces. It comprises the proximal extremity and most of the shaft. The distal extremity is missing, as well as most of the radial tuberosity.

The Spy 15B right radius is composed of two fragments constituting most of the shaft situated under the radial tuberosity.

The Spy 7A left and 7B right ulnae are represented by the proximal extremity and the part of the shaft bearing the brachialis muscle insertion. The olecranon of the 7B bone shows some damage on both olecranon process sides.

The Spy 15A left ulna proximal half is preserved, with however missing shards on both sides of the olecranon process and on the posterior side of the bone, behind the radial notch.

Because of the size difference existing between the 5B and 5A humeri on the one hand, and between the 14A and 14B humeri on the other hand, their respective association to the Spy 1 (representing individual Spy I) or to the more robust Spy 10 (representing individual Spy II) calvarium is straightforward. Similarly, the large size of the 15A and 7B ulnae suggests that they most likely belong to Spy II. In contrast, as further discussed below, the Spy 7A left ulna, traditionally attributed to Spy I, caught our attention because of its modern aspect which raised serious doubt on its affiliation to the Spy I Neandertal. Direct dating (Semal *et al.*, 2009, volume 1: chapter XVI) has indeed confirmed that it belongs to a Neolithic individual.

The attribution of the radii to Spy I or Spy II appears less obvious and has a fluctuating history (Rougier *et al.*, this volume: chapter XIX). Although Spy 6 (left side) has been attributed to Spy I, its dimensions are relatively large and close to those of Spy 15B (right side). Similarities between Spy 6 and Spy 15B are also apparent when their radiographies are examined (SF12 and SF13A). Longitudinal views of these two bones almost overlap, and their cross-sections show very comparable bone densities. This suggests that both radii could belong to the same individual, probably to the more robust Spy II Neandertal. The revised bone attribution is summarised in Table 1. The radii will however remain designated by their numbers (Spy 6 or Spy 15B) rather than by their hypothetical individual attribution (Spy II left or right).

The examination of the other human bones discovered at the Spy site, currently classified as Neolithic remains, led to set aside the Spy 336a right radius which exhibits Neandertal-like characters, as well as the Spy 181a left radius that could belong to the same individual. The Spy 336a radius comprises the radial neck, the radial tuberosity and the proximal part of the shaft, including the beginning of the interosseus border. The Spy 181a radius is a fragment composed of the radial tuberosity and of the most proximal part of the shaft and of the interosseus border. Although Spy 336a has recently been dated from the Neolithic period, both bones will be succinctly analysed in an attempt to improve the discrimination between Neandertal and modern human radii.

Individual	*Bone*	*Side*	*#*	*State of preservation*	*Length (mm)*
Spy I	Humerus	left	5B	Diaphysis	208
		right	5A	Diaphysis and distal extremity, medial epicondyle missing	206
	Ulna	*left*	*[7A]*	*Proximal quarter of the bone of a Neolithic individual*	*68*
Spy II	Humerus	left	14A	Diaphysis and distal extremity	243
		right	14B	Diaphysis and distal extremity, lateral epicondyle damaged	239
	Radius	left	6	Diaphysis and prox. extremity, radial tuberosity damaged	206
		right	15B	Diaphysis	147
	Ulna	left	15A	Proximal half of the bone	141
		right	7B	Proximal quarter of the bone	91

Table 1. State of preservation and individual attribution of the upper limb bones of the Spy Neandertals (original collection).

The humeri (Tables 2 and 3, Figure 1, SF2, SF3, SF5 and SF16)

The Spy humeri appear as rather slender with relatively widened distal extremities. The minimum perimeters (PH1: 5B = 55.0 mm, 5A = 57.0 mm, 14A = 59.0 mm, 14B = 67.0 mm) confirm a certain gracility of the bones with values inferior to the Neandertal (PH1 = 60.6 ± 6.9 mm) and modern (PH1 = 60.9 ± 6.6 mm) means, except for Spy II right (14B).

As observed by Thoma (1975), and like in other Neandertals (Vandermeersch, 1981; Trinkaus, 1983; Vandermeersch & Trinkaus, 1995; but see Heim, 1982), the Spy diaphyses are flattened in the medio-lateral direction. Their diaphyseal index (IH2: 5B = 68.3, 5A = 68.6, 14A = 70.5), except for Spy II right (14B = 79.0), is indeed low, inferior to the average value of the other Neandertals (IH2: N mean = 74.8 ± 6.0, MH mean = 78.9 ± 6.1).

The distal part of the biccipital groove is well-preserved on Spy I left (5B). It is rather wide (about 15 mm), bordered by well-defined, raised and smooth ridges of the greater (about 5.9 mm wide) and lesser tubercles (about 6.7 mm wide). The distal part of the crest of the greater tubercle is also visible on Spy 14A (about 9.3 mm wide) and 14B (about 7.6 mm wide) and the crest of the lesser tubercle is visible on 14A (Spy II left). All those muscle insertions show the same characteristics and allow to estimate the width of the biccipital groove of Spy II left (14A = 17 mm) and right (14B = 18 mm).

The Spy deltoid tuberosity (Figure 1a) is very narrow (IH5: 5B = 17.2, 5A = 20.8, 14A = 17.3, 14B = 20.0) and moderately developed (IH6: 5B = 94.8, 5A = 96.6, 14A = 95.3, 14B = 98.5). These features are common among Neandertals (Endo, 1971; Hambücken, 1993a, 1993b; Churchill & Smith, 2000) (IH5 = 22.2 ± 3.3 and IH6 = 96.2 ± 2.2), while, on average, the modern deltoid tuberosity is wider and more developed (IH5 = 27.0 ± 2.3 and IH6 = 94.2 ± 3.1). Its distal limit seems to be very low in Spy 5B.

In modern humans, the anterior crest of the deltoid tuberosity is typically in continuity with the greater tubercle crest, and both are parallel to the bone shaft, generally forming the proximal part of the anterior border. On Spy I left and right (5B and 5A) and Spy II left (14A), the crest of the greater tubercle is indeed parallel to the shaft, but the anterior deltoid tuberosity crest deviates from the bone axis and meets it only at its distal extremity. As a result, the tuberosity forms a large and very slight curve with a lateral convexity, totally deported to the lateral face of the bone. This structure is therefore almost invisible in anterior view. This morphology is particularly marked in Spy 5B (Figure 1a). On these three bones, there is therefore a medio-anterior face instead of an anterior border. This medio-anterior face is slightly convex and wide whereas the medial face is usually flat among modern humans.

Humerus			*Spy I*		*Spy II*		*Neandertals*		*Modern Humans*	
			5B	*5A*	*14A*	*14B*				
Measurements	*Description*	*Author*	*left*	*right*	*left*	*right*	*n*	*m ± s*	*n*	*m ± s*
PH1 (mm)	shaft minimum perimeter	M7	55.0	57.0	59.0	67.0	20	60.6 ± 6.9	400	60.9 ± 6.6
PH3	deltoid tuberosity perimeter 5/12 level	Endo, 1971	58.0*	59.0*	62.0*	68.0*	18	64.2 ± 6.5	370	64.6 ± 7.5
DH1	shaft maximum diameter	M5	20.8	21.0	21.7	22.4	20	21.3 ± 2.3	368	21.4 ± 2.5
DH2	shaft minimum diameter	M6	14.2	14.4	15.3	17.7	18	16.2 ± 2.3	368	16.8 ± 2.1
WH1	deltoid tuberosity width 5/12 level	Endo, 1971	10.0*	12.3*	10.7*	13.6*	18	**14.2 ± 2.2**	361	**17.5 ± 2.8**
WH4	distal extremity width	M4	-	-	65.0	-	19	**61.7 ± 4.4**	321	**57.9 ± 5.9**
WH7	medial pillar width		-	6.6	-	10.0	33	**8.1 ± 1.8**	392	**10.9 ± 2.2**
WH8	lateral pillar width		-	15.1	18.2	19.7	28	**15.4 ± 2.6**	356	**17.3 ± 2.5**
WH9	medial epicondyle width		-	-	20.0	20.0	21	**20.3 ± 2.0**	310	**18.4 ± 2.9**
WH10	lateral epicondyle width		-	-	6.0	-	20	**5.3 ± 1.4**	309	**6.5 ± 1.9**
WH5	olecranon fossa width	M14	-	29.9	32.6	32.8	28	**29.4 ± 2.2**	373	**26.7 ± 2.4**
HH1	olecranon fossa height		-	23.9	24.9	24.3	30	**23.0 ± 1.6**	387	**20.5 ± 2.1**
FH2	olecranon fossa depth	M15	-	14.7	15.2	-	17	**14.6 ± 1.4**	330	**12.2 ± 1.9**
EH3	proximal limit of the coronoid fossa		-	23.0	27.0	28.0	26	**23.4 ± 2.4**	375	**25.5 ± 3.6**
EH4	proximal limit of the olecranon fossa		-	33.0	33.0	34.0	27	**32.7 ± 1.9**	381	**29.9 ± 2.9**
WH6	trochlear width (anterior face)	M11	-	22.5*	28.4*	27.7*	13	25.1 ± 2.9	275	24.2 ± 3.2
FH3	distal trochlear depth		-	3.0	2.1	3.0	26	2.7 ± 1.1	333	2.8 ± 0.7
DH6	capitulum sagittal diameter	M12	-	17.0	17.1*	-	21	16.9 ± 1.6	262	16.7 ± 1.9
DH7	capitulum transversal diameter		-	18.7	21.2	21.3*	20	19.1 ± 1.8	303	19.8 ± 2.0
AH1 (°)	epicondyle medial angle		-	-	5	8	16	12.9 ± 5.6	275	12.6 ± 6.9
AH4	anterior angle of the humeral pallet		-	37	67	74	30	**61.7 ± 12.4**	373	**72.0 ± 11.4**
AH6	trochlear angle / shaft axis		-	84	89	87	21	84.1 ± 2.4	310	82.6 ± 3.5

Table 2. Measurements of the Spy humeri. M stands for Martin (1914). * indicates that the measurement is estimated given the Spy fossil state of preservation. Values are compared to the Neandertals and modern humans means. Bold characters indicate significantly different means (Student's t-test, $p \leq 0.05$).

In most modern humans, the deltoid tuberosity crests clearly diverge in the proximal direction, the lateral crest quickly reaching the corresponding border of the shaft. This corresponds to the "open" morphology (as opposed to the "closed" morphology observed among Neandertals) described by Carretero *et al.* (1997). In Spy I left and right (5B and 5A) and Spy II left (14A), the crests appear as two juxtaposed, almost parallel and distally pointed crests. The anterior one is longer and more developed than the lateral one. The two crests are separated along their entire length by a narrow groove that tends to shrink distally. As a result, they do not really join as in most modern humans. In Spy I left and right (5B and 5A), the anterior crest is bordered medially by a small groove. A similar general shape can be observed in other specimens such as Neandertal 1.

Although the same curved morphology is present on Spy II right (14B), the crests are wider, and the anterior one is more parallel to the shaft, more visible in anterior view, and thus less laterally deported. Three of the Spy humeri (5B, 5A and 14B) moreover display a third crest between the two main ones. On Spy 14A, the presence of a third crest is more disputable, even if a small ridge can be seen in the central part of the tuberosity. The Spy third crest appears as thin, slightly raised and well-defined while it is usually wider and more diffuse among modern humans.

The radial groove is shallow in Spy II and almost absent in Spy I. It appears rather highly placed as it seems to run all the way to the proximal limit of the lateral crest of the deltoid tuberosity. The radial groove causes shrinkage of the posterior face of the bone. The groove shows a rather angular lateral bound on Spy II right (14B) and especially on Spy II left (14A) and a more rounded one on Spy I, as a function of the groove depth. The posterior sides of the bones are oblique in their proximal half (roughly through the distal limit of the deltoid tuberosity), especially on Spy 14B, giving to this bone a twisted aspect in comparison with the approximately horizontal distal half of the shaft. In anterior view, the distal part of the Spy I right humeral shaft is high in the antero-posterior direction while the Spy II humeri are much flatter (AH4: 5A = 37°, 14A = 67°, 14B = 74°, N = 61.7 ± 12.4°, MH = 72 ± 11.4°).

The absolute width of the Spy II left distal extremity is very large (WH4: 14A = 65 mm, N = 61.7 ± 4.4 mm, MH = 57.9 ± 5.9 mm) reinforcing the perception of shaft slenderness. The humeral pallets are preserved in Spy I right (5A) and Spy II (14A and 14B). In continuity with the distal part of the shaft, the posterior face is flatter

Humerus			*Spy I*		*Spy II*		*Neandertals*		*Modern Humans*	
			5B	*5A*	*14A*	*14B*				
Indices	*Description*	*Author*	*left*	*right*	*left*	*right*	*n*	*m* ± *s*	*n*	*m* ± *s*
IH2 = DH2 % DH1	diaphyseal index	M&K	68.3	68.6	70.5	79.0	18	74.8 ± 6.0	368	78.9 ± 6.1
IH5 = WH1 % PH3	ind. of deltoid tuberosity width	Endo, 1971	17.2	20.8*	17.3*	20.0*	18	22.2 ± 3.3	361	27.0 ± 2.3
IH6 = PH1 % PH3	ind. of deltoid tuberosity development		94.8	96.6*	95.3*	98.5*	18	96.2 ± 2.2	368	94.2 ± 3.1
IH24 = WH7 % WH8	ind. of ratio between pillars		-	43.7	-	50.8	27	54.0 ± 9.4	344	63.0 ± 10.9
IH19 = WH5 % WH4	ind. of olecranon fossa width		-	-	50.2	-	17	48.4 ± 3.0	314	46.3 ± 3.9
IH20 = HH1 % WH5	ind. of olecranon fossa shape		-	79.9	76.4	74.1	27	75.6 ± 16.2	371	77.0 ± 7.9
IH21 = HH1 % WH4	ind. of olecranon fossa height		-	-	38.3	-	17	37.7 ± 2.7	317	35.3 ± 4.7
IH22 = FH2 % WH5	ind. of olecranon fossa depth		-	49.2	46.6	-	14	48.1 ± 4.8	329	45.9 ± 7.2
IH23 = EH3 % EH4	ind. of position of CF / position of OF		-	69.7	81.8	82.4	25	71.7 ± 7.0	375	85.3 ± 10.0
IH17 = WH9 % WH4	ind. of medial epicondyle width		-	-	30.8	-	14	33.4 ± 2.6	294	31.7 ± 3.9
IH18 = WH10 % WH4	ind. of lateral epicondyle width		-	-	9.2	-	14	8.6 ± 2.4	288	11.2 ± 2.9
IH29 = WH6 % WH4	ind. of trochlea width		-	-	43.7*	-	7	41.7 ± 2.4	255	41.6 ± 5.3
IH30 = FH3 % WH6	ind. of trochlea depth		-	-	7.4*	10.8*	8	12.5 ± 3.5	267	11.6 ± 3.0
IH25 = DH6 % WH4	ind. of capitulum width		-	-	26.3	-	12	27.2 ± 1.5	250	28.8 ± 3.6
IH28 = DH6 % DH7	ind. of capitulum shape		-	90.9	80.7*	-	14	88.6 ± 6.2	251	84.4 ± 8.3

Table 3. Indices of the Spy humeri. M&K stands for Martin & Knußmann (1980).
* indicates that the index is estimated given the Spy fossil state of preservation. Values are compared to the Neandertals and modern humans means. Bold characters indicate significantly different means (Student's t-test, p ≤ 0.05). Note that a high index does not always indicate a strong development.

than in most modern humans because of the very posterior position of the medial border. This border is very sharp in Spy 5A but it becomes distally blunter in Spy 14B (this area is destroyed in Spy 14A). The lateral borders are thin, sharp, and slightly rolled up in the anterior direction.

Figure 1. Upper limb bones of Spy I and Spy II in anterior view.
(a) Detail of the Spy 5B deltoid tuberosity in lateral view; (b) Detail of the Spy 6 radial tuberosity in medial view.
Note that the attribution of both radii to Spy II is hypothetical. Scale bars = 1 cm (Pictures by P. Semal, RBINS).

As in most Neandertals (IH24: N = 54.0 ± 9.4, MH = 63.0 ± 10.9), the Spy medial pillar appears thin in comparison with the lateral one (IH24: 5A = 43.7 and 14B = 50.8). This is particularly marked in Spy 5A, and artificially accentuated for Spy 14A because of a missing shard on the medial border.

The medial epicondyles are partially preserved on the Spy II humeri. Although they have been described as voluminous by Thoma (1975), they appear rather weakly developed (IH17: 14A = 30.8, N = 33.4 ± 2.6, MH = 31.7 ± 3.9) when compared to the distal width of the bones. The medial epicondyle is indeed usually more developed among Neandertals (Boule, 1911-1913; Smith, 1976; Heim, 1982; Trinkaus, 1983; Vandermeersch, 1991; Vandermeersch & Trinkaus, 1995).

Spy 14A medial epicondyle is rather trapezoidal, a common shape among modern humans (0 to 84.6 % depending on the sample, 29.2 % among Neandertals) while a more rounded shape is also observable among modern humans (6.7 to 100 % depending on the sample, n = 332), and while a rectangular and distally elongated medial epicondyle is frequent among the other Neandertals (70.8 %, n = 24) (Hambücken, 1993a). The medial epicondyles of the Spy II humeri however display well-marked insertions for the common tendon of the superficial flexor muscles of the forearm.

In comparison to the distal width, the lateral epicondyle development is moderate in Spy II left (IH18: 14A = 9.2). Although it is described as well-developed in La Chapelle-aux-Saints 1 (Boule, 1911-1913), Krapina (Smith, 1976) and Shanidar (Trinkaus, 1983), a low development index is commonly observed among Neandertals (IH18: N = 8.6 ± 2.4, MH = 11.2 ± 2.9). The maximum width of the lateral epicondyle is highly placed, just above the distal joint proximal limit. This morphology is common among Neandertals (Aiello & Dean, 1990), while modern humans display a maximum width often situated at the same level as the proximal half of the distal joint. The trace of the common tendon of the extensor muscles of the forearm is well-developed.

In accordance with the description of Thoma (1975), the Spy I and II olecranon fossae are large. They have been found equally large on several other Neandertals (Boule, 1911-1913; McCown & Keith, 1939; Smith, 1976; Vandermeersch, 1981, 1991; Heim, 1982; Vandermeersch & Trinkaus, 1995). It is in fact wide in comparison to the distal width (IH19: 14A = 50.2, N = 48.4 ± 3.0, MH = 46.3 ± 3.9), and rather deep (IH22: 5B = 49.2, 14A = 46.6) like in the other Neandertals (IH22 = 48.1 ± 4.8, MH = 45.9 ± 7.2). The Spy II fossae are wider in comparison with their height than the Spy I fossa (IH20: 5A = 79.9, 14A = 76.4, 14B = 74.1, N = 75.6 ± 16.2, MH = 77.0 ± 7.9). The proximal limit of the olecranon fossa is rounded in the Spy I right humerus (5A), while it is rather triangular in the Spy II humeri (14A and 14B).

As observed by de Lumley (1973) on the Neandertals of L'Hortus, the position of the Spy olecranon fossa proximal limit is high in comparison with the proximal limit of the coronoid fossa as revealed by the low value of the "position" index (IH23: N = 71.7 ± 7.0, MH = 85.3 ± 10.0). Spy I right (5A) shows indeed a very low index (IH23 = 69.7), whereas the values of Spy II (IH23: 14A = 81.8, 14B = 82.4) are higher. There is no olecranon perforation on the Spy preserved olecranon fossae. The Spy II humeri however display one pin size hole on the right (14B) and two on the left (14A), bordered by a translucent patch revealing the thinness of the olecranon septum. The bottom of the Spy I right (5A) fossa is partially reconstructed, preventing a complete observation.

The Spy I and II coronoid fossae are relatively vast and deep. On the Spy II humeri, the area of the humeral pallet surrounding the coronoid fossa forms a raised and smooth crest originating from the anterior border of the distal shaft and bordering the medial side of the coronoid fossa. The lateral part of the humeral pallet is clearly lower and rougher (this area is unobservable on Spy I right [5A]). The Spy radial fossae appear as coarse and hollow areas.

The Spy II left capitulum is narrow (IH25: 14A = 26.3, N = 27.2 ± 1.5, MH = 28.8 ± 3.6) and ovoid. The long axis is slanted, bringing the maximum convexity of the structure in a proximo-lateral position. The capitulum is relatively highly placed in comparison with the trochlea.

While the Spy I right trochlea is rather narrow, those from Spy II are wide in comparison to the other Neandertals (WH6: 5A = 22.5 mm, 14A = 28.4 mm, 14B = 27.7 mm, N = 25.1 ± 2.9 mm, MH = 24.2 ± 3.2 mm). The relative width calculated on Spy II left confirms this observation (IH29: 14A = 43.7, N = 41.7 ± 2.4, MH = 41.6 ± 5.3). The borders of the medial trochlea of Spy II are massive and convex. The trochlea gorges are very shallow (IH30: 14A = 7.4, 14B = 10.8, N = 12.5 ± 3.5, MH = 11.6 ± 3.0).

The most proximal cross-sections (Figure 2, SF8 to SF11), obtained for Spy 5B, show well-marked and developed ridges of the lesser and greater tubercles. They reveal that the former is medially elongated, while the latter is anteriorly oriented. The proximal deltoid tuberosity sections of Spy 5A, 5B and 14A show a very developed anterior crest and a laterally oriented deltoid tuberosity. This lateral orientation is also visible on the middle and distal deltoid tuberosity sections. On the same sections, a third crest (on Spy 5A and 5B), a convex "anterior side" of the bone and a marked shaft flattening are also visible. The 14B deltoid tuberosity is less laterally oriented and its anterior crest is less developed.

The sections of the distal shaft are also markedly flattened in the medio-lateral direction, and consequently, the humeral pallet appears very high, especially on Spy 5B. The lateral borders are sharp and rolled up. The most distal sections mainly show a vast olecranon fossa.

The radii (Table 4, Figure 1, SF4)

As observed by Fraipont & Lohest (1887), the Spy 6 left radial head is small as indicated by a low articular perimeter (PR3: Spy 6 = 57.0 mm, N = 64.6 ± 4.8 mm and MH = 66.1 ± 6.1 mm). This is further confirmed when it is compared to the shaft minimum perimeter (IR20: Spy 6 = 71.9, N = 53.9 ± 2.7, MH = 59.3 ± 4.6). It seems however to be widened (IR21: Spy 6 = 57.9, while N = 53.5 ± 2.5 and MH = 63.5 ± 4.7), especially laterally, because of the great slenderness of the radial neck. This has been observed in other

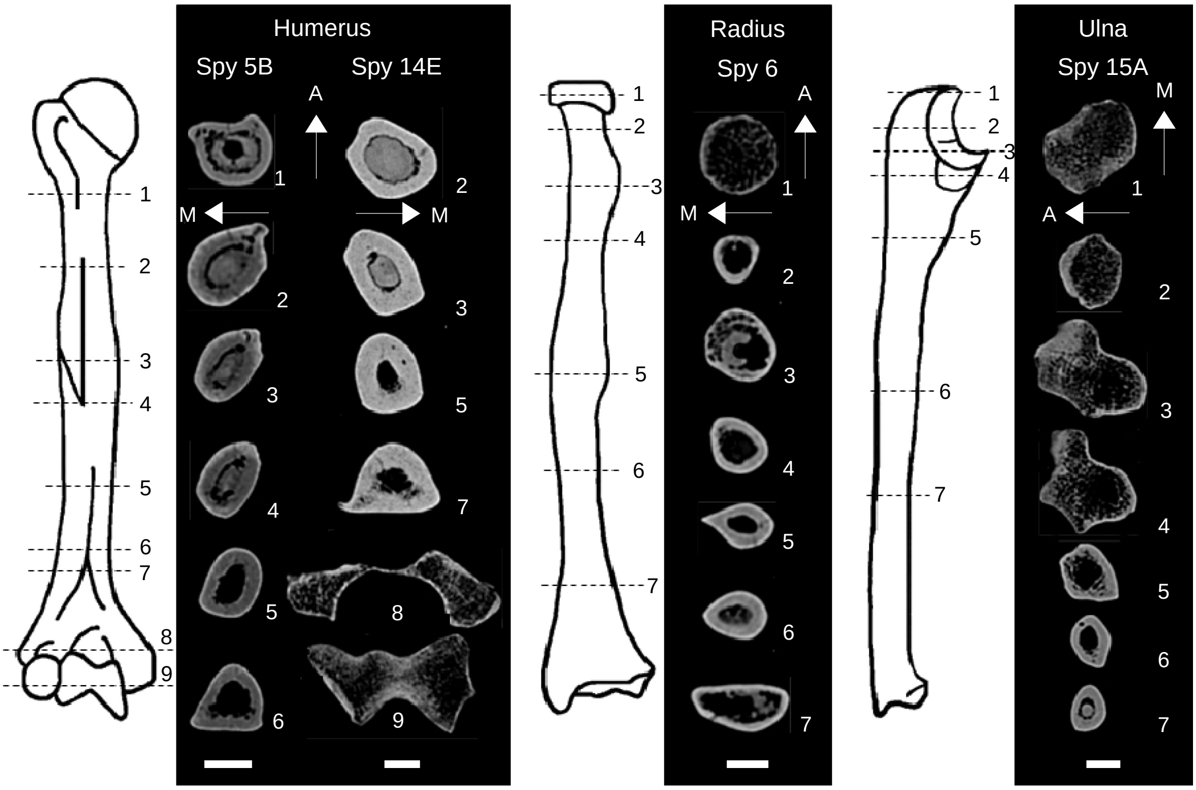

Figure 2. Cross-sections of the upper limb bones of Spy I and Spy II.
A: anterior direction; M: medial direction. Scale bars = 1 cm (Cross-sections processed by P. Semal, RBINS).

Neandertals as well (Boule, 1911-1913; Trinkaus, 1983). The radial head is circular (IR8 = 100.0) whereas it is most often slightly oval in the sagittal direction in Neandertals (IR8 = 96.8 ± 4.4) and modern humans (IR8 = 97.8 ± 2.9).

The radial fovea of the Spy 6 radius is shallow (IR11 = 6.7) like in most Neandertals (IR11: N = 8.2 ± 1.6, MH = 9.5 ± 1.7). While in modern humans the proximal articular periphery usually shows a marked difference between its maximum and minimum heights, as revealed by a low index (IR10 = 38.2 ± 10.2), such values are much closer in Neandertals (IR10 = 58.4 ± 11.4). Spy 6 is no exception, with a particularly high index (IR10 = 64.4).

The Neandertal radial neck is sometimes described as being long (Boule, 1911-1913), but most often as variable in length (Vandermeersch, 1981, 1991; Heim, 1982; Trinkaus, 1983). It appears a little longer in Neandertals (LR3 = 31.9 ± 2.8 mm) than in modern humans (LR3 = 30.2 ± 3.0 mm). The length of the radial neck of the Spy 6 radius can be evaluated as being 38.0 mm. However, since it is measured from the proximal extremity to the center of the radial tuberosity, this value might be overestimated in Neandertals because of the height of the articular perimeter and the large size of the radial tuberosity of some of them. In Spy 6 case, this impression is also reinforced by the thinness of the radial neck. The perimeter of the Spy 6 neck is indeed particularly low (PR4: Spy 6 = 33.0 mm, N = 35.7 ± 4.0 mm, MH = 42.8 ± 4.6 mm). Although this perimeter can be either inferior or superior to the minimum perimeter, it tends to be lower in Neandertals as revealed by an average index higher than 100 (IR14 = 101.9 ± 8.7) while the opposite pattern tends to be observed in modern humans (IR14 = 91.2 ± 16.8). The particularly high index calculated for the Spy 6 radius (IR14 = 124.2) confirms the important slenderness of the neck. The Spy 6 radial neck is also very flattened transversely (IR22: Spy 6 = 109.0, N = 105.5 ± 12.9, MH = 106.1 ± 7.6) with a flat lateral side.

Although damaged, the radial tuberosity of Spy 6 has been described by Fraipont & Lohest (1887) as a trough bordered by rough lips. Its outlines are sufficiently preserved to delineate a very vast structure, approximately 30 mm long (without the anterior radial tuberosity extension, see below) and 15 mm wide. Even though a large muscle insertion can be observed on the right side of Neandertal 1 or on the left side of Shanidar 4 for example, and although Churchill (1994) has highlighted the great size of this structure in Neandertals in general, the Spy 6 radial tuberosity appears unusually long. Measures taken on a partial sample of ten Neandertal radii (La Chapelle-aux-Saints 1, La Ferrassie 2, Regourdou 1, Neandertal 1, Krapina, Tabun C1, Shanidar 4, 6 and 8) indeed indicate an average length of 20.3 ± 3.0 mm and an average width of 13.3 ± 2.0 mm. Although the length might be overestimated because of the bone restoration, the Spy value is clearly outside the range of variation of the other Neandertals. Unfortunately, the poor state of preservation of the radial tuberosity of Spy 6 prevents further examination to determine if its size is of pathological origin.

Contrary to the radial tuberosity of modern humans which is sometimes distally well-defined and separated from the shaft by a well-marked convexity, the Spy 6 tuberosity extends distally in its anterior part and blends to the shaft (Figure 1b). This morphology is also present on individuals such as La Ferrassie 1 and 2, Neandertal 1, Regourdou 1, Shanidar 4 and 6, La Quina 5 and Tabun C1. The same morphology is however frequently observed in Upper Palaeolithic individuals as well (personal observation).

The Spy 6 radial tuberosity is relatively medially situated, as a virtually extended interosseus border would cut it in its anterior part. This relatively medial situation (55.6 %) or an even more medial one (cut in half by the interosseus border, 44.4 %, n = 18) is frequent among Neandertals (Boule, 1911-1913; McCown & Keith, 1939; Patte, 1955; Smith, 1976; Vandermeersch, 1981, 1991; Heim, 1982; Trinkaus, 1983; Trinkaus & Churchill, 1988) and is also observed among modern humans with a more variable frequency (respectively 9.1 to 81.0 % and 0 to 18.2 % depending on the sample). An anteriorly placed tuberosity is absent in the currently known Neandertals, but quite frequent in modern populations (9.5 to 90.9 %, n = 392) (Hambücken, 1993a).

Fraipont & Lohest (1887) described the Spy shaft of the radius as gracile. The Spy 6 radius has however a high minimum perimeter (PR1: Spy 6 = 41.0 mm, N = 36.9 ± 4.8 mm and MH = 40.0 ± 4.4 mm).

The Spy 6 shaft is almost straight in medial view. As pointed out by Fraipont & Lohest (1887) and Thoma (1975), the Spy radii shafts display a strong bending in anterior view (AR2: Spy 6 = 163°, 15B = 162°). This type of bending has been described in other Neandertals (Boule, 1911-1913; Patte, 1955; Smith, 1976; Vandermeersch, 1981, 1991; Vandermeersch & Trinkaus, 1995) (AR2: NH = 165.8 ± 6.1º, MH = 172.6 ± 2.6º). In contrast, the Spy 6 colo-dia-

Radius			*Spy II*		*Neandertals*		*Modern Humans*	
			6	*15B*				
Measurements/ Indices	*Description*	*Author*	*left*	*right*	*n*	*m ± s*	*n*	*m ± s*
PR1 (mm)	shaft minimum perimeter	M3	41.0	-	18	**36.9 ± 4.8**	366	**40.0 ± 4.4**
DR3	shaft sagittal diameter at DR4 level	M5	10.7	11.3	14	11.0 ± 1.2	377	11.5 ± 1.5
DR4	shaft maximum transversal diameter	M4	15.9	17.8	14	15.7 ± 1.9	377	15.5 ± 1.8
LR3	radial neck length		38.0*	-	20	**31.9 ± 2.8**	350	**30.2 ± 3.0**
PR4	radial neck perimeter	M5(4)	33.0	-	23	**35.7 ± 4.0**	346	**42.8 ± 4.6**
DR7	radial neck sagittal diameter	M5(2)	10.9	-	22	**11.6 ± 1.4**	356	**13.9 ± 1.6**
DR8	radial neck transversal diameter	M4(2)	10.0	-	22	**11.1 ± 1.4**	355	**13.1 ± 1.6**
PR3	proximal articulation perimeter	M5(3)	57.0	-	8	64.6 ± 4.8	142	66.1 ± 6.1
DR5	proximal articulation sagittal diameter	M5(1)	17.9	-	11	21.0 ± 1.8	179	21.0 ± 2.0
DR6	proximal articulation transversal diameter	M4(1)	17.9	-	15	20.3 ± 2.2	201	20.6 ± 2.0
FR1	fovea radii depth		1.2	-	20	**1.7 ± 0.4**	294	**2.0 ± 0.4**
HR1	maximal height of the prox. articular perimeter		8.7	-	16	**8.9 ± 1.4**	316	**9.6 ± 1.4**
HR2	minimal height of the prox. articular perimeter		5.6	-	6	**5.3 ± 0.9**	149	**3.6 ± 0.8**
PR5	radial tuberosity perimeter		-	-	21	**44.5 ± 6.1**	359	**49.4 ± 5.7**
ER2	interosseus border distal limit		114.9	-	9	**109.6 ± 6.4**	321	**143.3 ± 22.3**
AR1 (°)	colo-diaphyseal angle	M7	175.0	-	13	**167.3 ± 4.3**	328	**171.3 ± 4.4**
AR2	diaphyseal curvature angle	M6d	163.0	162.0	13	**165.8 ± 6.1**	323	**172.6 ± 2.6**
IR2 = DR3 % DR4	diaphyseal index	M&K	67.3	63.5	14	**70.2 ± 5.5**	376	**74.4 ± 8.0**
IR20 = PR1 % PR3	ind. of proximal development		71.9	-	3	**53.9 ± 2.7**	136	**59.3 ± 4.6**
IR21 = PR4 % PR3	ind. of proximal development / neck		57.9	-	8	**53.5 ± 2.5**	141	**63.5 ± 4.7**
IR12 = LR3 % PR4	ind. of neck robusticity		115.2	-	10	**96.2 ± 13.7**	334	**71.0 ± 8.1**
IR14 = PR1 % PR4	ind. of radial neck development		124.2	-	16	**101.9 ± 8.7**	345	**91.2 ± 16.8**
IR22 = DR7 % DR8	ind. of radial neck section		109.0	-	22	105.5 ± 12.9	352	106.1 ± 7.6
IR15 = PR1 % PR5	ind. of radial tuberosity development		-	-	16	81.8 ± 6.2	351	81.4 ± 4.8
IR8 = DR6 % DR5	ind. of proximal extremity shape		100.0	-	9	96.8 ± 4.4	157	97.8 ± 2.9
IR10 = HR2 % HR1	ind. of circumferencia articularis shape		64.4	-	5	**58.4 ± 11.4**	148	**38.2 ± 10.2**
IR11 = FR1 % DR6	ind. of fovea radii depth		6.7	-	11	**8.2 ± 1.6**	188	**9.5 ± 1.7**

Table 4. Measurements and indices of the Spy radii. Abbreviations and codes as in Table 3.

physeal angle is very open (AR1: Spy 6 = 175º) whereas it is usually more acute in Neandertals and even in modern humans (AR1: NH = 167.3 ± 4.3º, MH = 171.3 ± 4.4º). The low colo-diaphyseal angle observed in Spy 6 could be explained by the necessity to accommodate its very massive radial tuberosity in the interosseus space.

The shaft is very flattened in the antero-posterior direction in Spy 6 (IR2 = 67.3) as well as in Spy 15B (IR2 = 63.5). This flattening, noted by several authors on other Neandertals (McCown & Keith, 1939; Smith, 1976; Vandermeersch, 1981; Heim, 1982) is confirmed by their low average index (IR2: N = 70.2 ± 5.5, MH = 74.4 ± 8.0).

The Spy 6 (left) interosseus border is moderately developed, but bordered by a concave area on the posterior side of the bone. The concavity is shallower in Spy 15B (right). In comparison with the average situation observed in modern humans, the interosseus border is short in Spy 6 (ER2 = 114.9 mm) and especially in Spy 15B. A short interosseus border is commonly observed in Neandertals (ER2: N = 109.6 ± 6.4, MH = 143.3 ± 22.3), although it as been described in various ways (Endo & Kimura, 1970; Smith, 1976; Heim, 1982; Trinkaus, 1983; Vandermeersch, 1991; Vandermeersch & Trinkaus, 1995). Like in most Neandertals, the interosseus tubercle is absent in Spy (it is absent or weakly developed in 80.0 % of the Neandertals, n = 20; Hambücken, 1993a).

In Spy, the insertions for the pronator teres are well-defined, long and slightly raised. They are approximately 27.3 mm long and 5 mm wide on Spy 6 (left), and 25.8 mm long and 6.8 mm wide on Spy 15B (right). They are located near the maximum bending point of the shaft.

Although it has recently been dated from the Neolithic period, a proximal portion of a right radius found at the same site, Spy 336a, shows some features evoking the Neandertal morphology (ST3, SF7 and SF15A). The radial tuberosity is indeed in a medial position as compared to the interosseus border. The perimeter of the Spy 336a radial neck (PR4 = 38.0 mm) is higher than in Spy 6 (PR4 = 33.0 mm), but still moderately developed in comparison to the minimum perimeter (IR14 = 97.4). The radial neck is very flattened transversely (IR22 = 108.9). Both indices are within the Neandertal variability, and outside the Spy and Mosan Neolithic cluster, although the overlapping with modern humans is important (SF15A). Like in most Neandertals, the Spy 336a radial tuberosity is much smaller (approximately 17 mm long and 11 mm wide) than that of the Spy 6 radius. It is rather weakly developed in absolute (PR5: 336a = 43.0 mm, N = 44.5 ± 6.1 mm, MH = 49.4 ± 5.7 mm) and relative value (IR15: 336a = 86.0, N = 81.8 ± 6.2, MH = 81.4 ± 4.8). The shaft minimum perimeter is high (PR1 = 37.0 mm). Unlike the Spy 6 radius, Spy 336a displays a slight angle in medial view.

The dimensions and aspect of the left fragmentary Spy 181a radius, found at the same site, are close to those of Spy 336a and both are part of the Neandertal cluster (SF15A, panel c), but outside the Spy and Mosan Neolithic variability. They could in fact belong to the same individual. Their radial tuberosity morphology looks like that of Spy 6, displaying an antero-distal convexity extension that blends with the shaft, and differs from that of the Mosan and Spy Neolithics which is well-developed and distally well-defined. However, only Spy 336a shows a medially placed tuberosity, clearly evoking a possible Neandertal affiliation (this situation is observed in only 0 to 18.3 % of the modern samples, n = 392). If both radii come from the same individual, it is thus unlikely that they belong to a Neandertal, in this case, to Spy I. Spy 181a has indeed an anteriorly oriented radial tuberosity which is currently unknown in Neandertals, but quite common in modern samples (9.5 to 90.9 %, n = 392; Hambücken, 1993a). This illustrates the difficulty to differentiate between Neandertals and modern humans when the remaining parts of the bone are not the most distinctive. Dating was therefore necessary to definitively make a decision about the taxonomic affiliation of Spy 336a and 181a and to confirm that they belong to a “modern” individual.

The cross-section (Figure 2, SF12 and SF13A) taken at the proximal extremity of the Spy 6 radius confirms its rounded shape. The section of the radial neck exhibits three flattened faces, while the radial tuberosity section highlights its partially medial orientation. The minimum perimeter level also displays a triangular-like shape. On the most distal sections, both Spy 6 and 15B show a posterior concavity next to the interosseus border.

The ulnae (Table 5, Figure 1, SF6 and SF16)

As observed by Boule (1911-1913), Patte (1955) or Vandermeersch (1981) on various Neandertals, the ulna proximal extremities of Spy II are voluminous as revealed by their width (WU1: 15A = 34.0 mm, 7B = 35.0 mm, N = 28.7 ± 5.7 mm, MH = 26.3 ± 3.8 mm). The Spy II left proximal extremity is very bent in the anterior direction in comparison to the shaft axis (AU6: 15A = 169°, N = 168.0 ± 3.0°, MH = 171.8 ± 4.6°).

The Spy olecranon is wide (WU2: 15A = 31.7 mm, N = 25.5 ± 2.7 mm, MH = 23.8 ± 2.7 mm), and thin in the antero-posterior direction (IU13: 15A = 82.0, 7B = 78.9, N = 79.7 ± 10.2, MH = 94.8 ± 14.3). It is also relatively long in comparison with the depth of the olecranon process (IU16: 15A = 81.5, 7B = 83.7, N = 80.5 ± 6.6 and MH = 77.8 ± 10.2).

In posterior view, the insertions for the triceps brachialis and anconeus muscles are well-marked, especially on the right side (7B). When observed in lateral view, the olecranon is well-visible while it is most often hidden “behind” the coronoid notch in modern humans (Hambücken, 1993a). On the left side (15A), it is proximally rounded, with, however, a slightly distally oriented axis and a small posterior edge corresponding to the most prominent part of the insertion for the triceps brachialis. In contrast, the olecranon top is slightly rounded on the left side, with a general horizontal axis.

The Spy olecranon processes are well-developed (HU1: 15A = 29.1 mm, 7B = 29.3 mm) when compared to the Neandertal average (HU1: N = 26.9 ± 2.1 mm, MH = 24.0 ± 2.5 mm). The Spy II coronoid processes are long in absolute value (HU2: 15A = 34.6 mm, 7B = 35.2 mm, N = 31.1 ± 3.0 mm, MH = 33.4 ± 3.4 mm), but faintly projected in comparison with the olecranon process. The index comparing both dimensions is indeed high (IU14: 15A = 84.2, 7B = 83.2) like in the other Neandertals (IU14: N = 84.7 ± 3.6, MH = 71.6 ± 5.8). Because of the faint projection of the coronoid process, the trochlear notch is anteriorly oriented in Spy II and in the other Neandertals while it is more proximally turned in modern humans. This is confirmed by the acute trochlear angle (AU4: 15A = 19º, 7B = 18º, N = 22.0 ± 8.9º, MH = 29.3 ± 17.7º) formed by a line joining the olecranon and coronoid process and the axis of the proximal extremity in lateral view. The tip of the coronoid process is horizontal as observed in other Neandertals (Boule, 1911-1913; Patte, 1955; Vandermeersch, 1981). It is in fact horizontal or distally oriented in 95.8 % of the Neandertals (n = 24) and in 0 to 93.3 % of modern populations, depending on the sample (n = 363; Hambücken, 1993a). A proximally oriented coronoid process is however usually predominant among modern humans.

In Neandertals, the difference between the maximum and minimum widths of the trochlear notch is more marked than in modern humans (IU21: N = 60.5 ± 11.4, MH = 74.7 ± 9.3). This feature is particularly visible on the Spy II ulnae (IU21: 15A = 56.1) although damage to the right side prevents accurate measurement.

The relief under the coronoid process is very concave and abrupt in Spy II (see also Fraipont & Lohest, 1887; Thoma, 1975). This morphology is more often observed in Neandertals (54.2 %, n = 24) than in modern humans (0 to 20.0 % of the bones depending on the sample, n = 354; Hambücken, 1993a). The connection between the coronoid process and the shaft is indeed more progressive in most modern humans.

The Neandertal radial notch has been described in various ways (Boule, 1911-1913; McCown & Keith, 1939; Patte, 1955; Smith, 1976; Vandermeersch, 1981). According to Fraipont & Lohest (1887), it is vast and oblique in Spy. It is indeed oriented sideways as revealed by the very obtuse angle formed between the axis of the radial notch and the transversal axis of the trochlear notch (AU3: 15A = 117º and 7B = 115º). This angle is indeed more open in Neandertals than in modern humans on average (AU3: N = 96.1 ± 19.4º, MH = 88.2 ± 21.2º). The posterior side of the radial notches leans against the supinator crest.

The Spy II radial notches are moderately high, particularly on the left (IU20: 15A = 81.5, 7B = 90.4) as compared to the other Neandertals (IU20 = 93.8 ± 20.8) although higher than in modern humans (IU20 = 64.5 ± 11.4). The left side has a roughly parallelogram shape with a

Ulna			*Spy II*		*Neandertals*		*Modern Humans*	
			15A	*7B*				
Measurements/ indices	*Description*	*Author*	*left*	*right*	*n*	*m ± s*	*n*	*m ± s*
DU3 (mm)	sagittal diameter of the proximal shaft	M14	21.8	22.9	10	**19.7 ± 2.9**	354	**21.9 ± 3.0**
DU4	transversal diameter of the proximal shaft	M13	25.2	24.1	10	19.2 ± 2.6	350	19.1 ± 2.6
DU5	olecranon thickness	M7b	19.4	19.3	5	17.7 ± 3.3	329	17.4 ± 1.7
WU1	proximal width	M6(1)	34.0	35.0	6	**28.7 ± 5.7**	313	**26.3 ± 3.8**
WU2	olecranon width	M6	31.7	-	11	**25.5 ± 2.7**	257	**23.8 ± 2.7**
HU1	olecranon process depth	M7c	29.1	29.3	7	**26.9 ± 2.1**	301	**24.0 ± 2.5**
HU2	coronoid height	M7d	34.6	35.2	14	**31.1 ± 3.0**	286	**33.4 ± 3.4**
HU3	olecranon height	M8	23.7	24.5	10	**22.0 ± 2.3**	331	**18.6 ± 2.6**
HU4	olecrano-coronoid height		27.5	24.0	6	**25.1 ± 1.5**	274	**23.2 ± 2.5**
WU3	trochlear notch maximum width	M6b	26.9	-	8	24.7 ± 3.1	256	23.3 ± 2.5
WU4	trochlear notch minimum width	M6a	15.1	16.8	13	**14.5 ± 2.4**	320	**17.3 ± 2.3**
RU2	trochlear notch arc		36.0	36.0	8	35.3 ± 7.1	262	34.4 ± 3.6
WU5	pars coronoidea medial width		14.9	15.3	12	13.5 ± 1.3	308	13.6 ± 1.9
WU6	pars coronoidea lateral width		9.8	10.2	15	9.4 ± 1.2	350	8.7 ± 1.3
WU7	radial notch width	M9a	13.0	11.5	16	12.4 ± 2.2	292	16.0 ± 2.1
HU7	radial notch height	M9b	10.6	10.5	17	11.4 ± 1.7	331	10.2 ± 1.4
AU3 (°)	radial notch / trochlear notch angle	Heim, 1982	117.0	115.0	13	96.1 ± 19.4	306	88.2 ± 21.2
AU4	trochlear angle	M15a	19.0	18.0	8	22.0 ± 8.9	270	29.3 ± 17.7
AU6	proximal extremity / shaft axis		169.0	-	13	**168.0 ± 3.0**	306	**171.8 ± 4.6**
IU6 = DU4 % DU3	ind. of platoleny (Verneau)		115.6	105.3	17	**97.9 ± 10.2**	346	**87.8 ± 12.2**
IU13 = DU5 % HU3	ind. of olecranon thickness		82.0	78.9	6	**79.7 ± 10.2**	316	**94.8 ± 14.3**
IU16 = HU3 % HU1	ind. of olecranon shape		81.5	83.7	7	80.5 ± 6.6	291	77.8 ± 10.2
IU14 = HU1 % HU2	ind. of coronoid process development		84.2	83.2	6	**84.7 ± 3.6**	254	**71.6 ± 5.8**
IU21 = WU4 % WU3	ind. of trochlear notch shape		56.1	-	6	**60.5 ± 11.4**	253	**74.7 ± 9.3**
IU19 = HU4 % RU2	ind. of trochlear notch concavity		76.4	66.5	5	**74.2 ± 5.5**	248	**67.6 ± 4.7**
IU22 = WU6 % WU5	ind. of pars coronoidea width		65.8	66.8	11	**71.2 ± 8.2**	305	**64.1 ± 9.8**
IU20 = HU7 % WU7	ind. of radial notch shape		81.5	90.4	15	**93.8 ± 20.8**	288	**64.5 ± 11.4**

Table 5. Measurements and indices of the Spy ulnae. Abbreviations and codes as in Table 3.

rounded disto-posterior angle. The same shape is observable on the right, with however a small notch in the proximo-posterior corner.

The Spy II supinator crests, situated under the distal limit of the radial notch, are fairly developed. The crest is very short on the left side (15A [it is only observable in its very proximal part on the right, 7B]) and separated by a convex area from the longitudinal crest of the shaft latero-posterior face. In modern humans these crests are usually aligned. In Spy, the crest that borders the well-marked insertion for the long abductor muscle of the thumb is sharp in its proximal part.

Like in most Neandertals (78.9 %, n = 19), there is no hollow for play of the radial tuberosity in the Spy II ulnae, while a depression is observable in 0 to 53.8 % of modern humans (n = 360; Hambücken, 1993a).

The 15A (left) ulna proximal shaft appears relatively slender. The area situated under the coronoid process (it is measured just under the radial notch level) is usually considered as being flattened in Neandertals (Boule, 1911-1913; Patte, 1955; Endo & Kimura, 1970; Vandermeersch, 1981). The platoleny indices of Spy II are particularly high (IU6: 15A = 115.6, 7B = 105.3, N = 97.9 ± 10.2, MH = 87.8 ± 12.2) indicating indeed a very low sagittal diameter. The insertion marks for the brachialis muscle are well-defined and distally raised, especially on the right side (7B). It is, however, largely stuck to the shaft, and not placed on a prominent area like in most modern humans.

The 15A (left) anterior face of the ulna is slightly convex. The longitudinal crest separating the postero-lateral side in two areas is well-visible but becomes distally blunter. The posterior border is sharp in its proximal part, from the distal olecranon zone to the three-quarter of the remaining length. It then becomes rounder and virtually disappears. The 15A interosseus border is a simple angulation (it is absent to moderately developed in 96.3 % of the Neandertals, n = 27, and in 23.1 to 100 %, n = 351, of modern humans, depending on the sample; Hambücken, 1993a). It has indeed been often described as being rather blunt in most Neandertals (Endo & Kimura, 1970; Thoma, 1975; Smith, 1976; Trinkaus, 1983).

The Spy 7A ulna (ST3, SF5B and SF15B), which has recently been dated from the Neolithic period (Semal *et al.*, 2009), indeed shows a modern aspect. The proximal shaft flattening is moderate (platoleny index: IU6 = 91.2). The trochlear notch is proximally oriented (AU4 = 26°), with a well-developed coronoid process (IU14 = 70.3). The olecranon is thick in the antero-posterior direction (IU13 = 98.2). Its top is hidden by the trochlear notch in lateral view. In anterior view, the trochlear notch shows no marked shrinkage in its middle part (IU21 = 78.6), and the bone relief under the coronoid process is progressive and does not exhibit any concave area. Finally, the radial notch is vertically oriented. Except for the platoleny index (IU6), the other indices of the Spy 7A ulna, the development of the coronoid process (IU14) and the trochlear notch shape (IU21), clearly stick out the Neandertal variability and situate this bone within the Mosan and Spy Neolithics cluster (SF15B).

The cross-sections (Figure 2, SF13B and SF14) comparison of the Spy II (15A and 7B) ulnae with Spy 7A is interesting since the latter belongs to a Neolithic individual and enables a comparison between the two taxa. The olecranon process section is larger in Spy 15A and 7B than in 7A because of the larger development of the olecranon above the trochlear notch level often observed among Neandertals. The Spy 7A olecranon thickness is more important at the trochlear notch level than in Spy 15A and 7B. The coronoid process section has an oblique shape and an oblique radial notch in Spy 7B and 15A while both the coronoid process and the radial notch are parallel to the sagittal axis in Spy 7A. The same cross-section reveals a marked protuberance on the lateral side of 7B and 15A, corresponding to the coronoid tubercle. The next sections, taken at the radial notch level, further highlight the coronoid tubercle protuberance and oblique radial notch orientation of the Spy II ulnae. These sections also show a rounded posterior side which is more pointed on 7A. The section taken at the brachialis level indicates an anterior orientation of this insertion in 7A while the insertion is more medially oriented in Spy II ulnae. These sections also display a better defined and crisp shape in Spy 7A, with sharp borders, particularly for the supinator crest. The most distal sections are only preserved on Spy 15A, and appear rounded, without the sharp edges usually visible on modern human shafts.

VARIABILITY

Spy I and Spy II dimorphism

The size difference between Spy I and Spy II is marked and clearly visible on the humeri. Although Spy I has sometimes been attributed to a female and Spy II to a male, in the absence of innominate bones, their sex attribution remains disputed (Fraipont & Lohest, 1887; Sollas, 1907; Morant, 1927; Thoma, 1975; Smith, 1980; Trinkaus, 1980; Ben-Itzhak *et al.*, 1988).

As shown in ST2, the Spy II humeri and ulnae values are included in the range of variation of the European male Neandertals, except for the left side deltoid tuberosity width, which is lower. As far as the radii are concerned, Spy 6 and 15B dimensions are comprised within the male variation interval, although the left side values are relatively low. The perimeter of the Spy 6 neck (PR4), however, appears as being particularly weak, even in comparison with the La Ferrassie 2 female. The Spy I dimensions are situated outside the range of variation of the European males, and globally close to the La Ferrassie 2 female values (ST2). In addition, the degree of dimorphism calculated in Spy is comparable to the degree of sexual dimorphism (female mean value / male mean value X 100) calculated for the humeral shaft dimensions of some of the modern samples. It is close as well to the sexual dimorphism calculated between the Neandertals of La Ferrassie on the one hand, and of Kebara and Tabun on the other hand (Figure 3).

Despite the scarcity of reference individuals, the comparison of the Spy upper limb fossils to the sexed European Neandertals, as well as their degree of dimorphism, would thus be consistent with the attribution of Spy II to a male, and probably of Spy I to a female. Although the study of the upper limb remains insufficient to allow a reliable sex determination, this would explain the marked size difference observed between the Spy individuals.

Position of the Spy fossils within Neandertal variability

The upper limb bones of the Spy Neandertals are generally well-integrated in the West-European Neandertal sample. Considering our limited perception of the actual Neandertal variability, it is not surprising that the Spy fossils show features that seem to stick out from the typical morphology currently established for their taxon. For example, Spy II shows relatively weakly developed and trapezoid shaped medial epicondyles and the radial tuberosity is in a less medial position than in most Neandertals. On the other hand, this

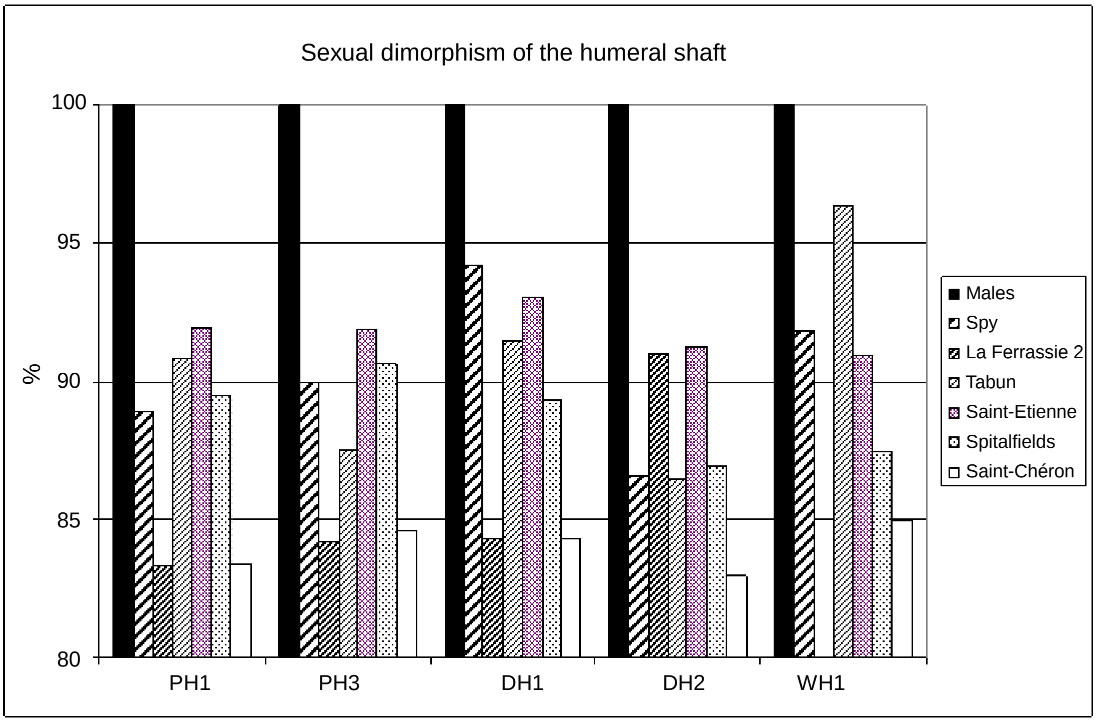

Figure 3. Sexual dimorphism of the humeral shaft. Males, either Neandertal or modern, are considered as the reference (100 %, black bars). Dimensions of the females are expressed as the percentage of those of the males (average female value / average male value X 100). PH1: minimum perimeter of the shaft; PH3: perimeter at the 5/12 of the bone maximum length; DH1: maximum diameter of the shaft; DH2: minimum diameter at the same level; WH1: deltoid tuberosity width at the PH3 level. Note that the La Ferrassie 2 value for WH1 (58.1) does not appear on the figure as it falls way below the interval of variation of the other samples.

individual also shows particularly marked Neandertal tendencies such as a very slender neck and a very homogeneous height of the proximal articular periphery on the radius, as well as a particularly short coronoid process of the ulna. Finally, the most distinctive features shared by the Spy Neandertals (particularly by Spy 5B, 5A and 14A) are concentrated on the deltoid tuberosities of their humeri. These tuberosities are particularly narrow, slightly curved and placed laterally, and they exhibit three crests (on Spy 5B, 5A and 14B). Their anterior and lateral crests are well-defined and separated on their entire length by a narrow groove. The anterior crest is more developed and longer than the lateral one.

In modern humans, the deltoid tuberosity is usually composed of two crests (26.3 to 92.6 % of the bones depending on the sample) although a third one can be observed in many individuals (7.4 to 73.7 %, n = 383; Hambücken, 1993a). So far, only the Spy Neandertals show this third crest (Figure 1a) nested between the two main ones (Hambücken, 1997). Its aspect is however distinctive. It is a well-defined, narrow and slightly raised ridge while it is usually a diffuse elongated area in modern populations. This peculiar morphology, probably linked to the narrowness of the tuberosity, might be the reason for a certain discrepancy in the literature. Endo (1971) and Vandermeersch (1981) indeed considered that all Neandertals display a two-crest tuberosity while Thoma (1975) noted a third one on Spy I and on Regourdou 1. Carretero *et al.* (1997) observed a third crest on Atapuerca AT-93, attributed to *Homo heidelbergensis*.

According to Kobayashi (in Endo, 1971), it seems that, among modern Japanese populations, this third crest would appear only after the age of 30. This hypothesis has not been confirmed on other samples (Hambücken, 1993a). It is likely a non-pathological variation corresponding to the trace of the insertion of the middle section of the deltoid muscle (see the sketch published in Klepps *et al.*, 2004).

The narrowness of the Neandertal deltoid tuberosity has been pointed out by several authors (Endo & Kimura, 1970; Endo, 1971; Vandermeersch, 1981; Hambücken, 1993a, 1993b; Carretero *et al.*, 1997; Churchill & Smith, 2000). It is in fact a particularly marked feature common to the Spy humeri. A bivariate analysis comparing the deltoid tuberosity width with the shaft perimeter measured at the same level (Figure 4) indeed places three of the Spy humeri next to La Ferrassie 2 and to the left side of Neandertal 1 and La Quina 5. This proximity illustrates the extreme narrowness of the Spy tuberosity since La Ferrassie 2 is a female while the left upper limb of Neandertal 1 and La Quina 5 present proven or supposed pathologies (Martin, 1923; Trinkaus *et al.*, 1994) that could explain the small size of this structure due to developmental or use defect. There is however no satisfactory hypothesis to account for the narrowness of the Neandertal deltoid tuberosity (see the functional interpretation below). It seems that the width of the deltoid tuberosity is somewhat correlated with the other dimensions of the humeral shaft (Hambücken, 1993a). Churchill (1994), who compared the tuberosity width with dimensions of the upper body or of other humeral features, found the tuberosity distal limit to be the only significantly correlated measurement. Carretero *et al.* (1997) suggested a correlation between the angle of torsion of the humeral head and the tuberosity width. Such a correlation has been challenged by Churchill & Smith (2000). Whatever the signification of the deltoid tuberosity narrowness, these authors concluded that this feature is interesting in terms of phylogenic value since it is not directly linked to the body shape or to the degree of physical activity.

It is thus difficult to interpret the Spy deltoid tuberosities morphology, especially considering the limited knowledge we have about this structure in modern humans from an orthopaedic point of view (Klepps *et al.*, 2004). Their overall aspect however suggests that the Spy fossils represent an extreme of the currently known Neandertal variability. Various levels of curvature and lateral “deportation” can be observed on the deltoid tuberosities of other Neandertals (such as La Ferrassie 2 and La Quina 5 for example), which excludes the hypothesis of a local anomaly or distinctive feature, but none of them shows all the Spy characteristics. The closest shape can however be observed on the right humerus discovered at the Neandertal site (Hambücken, 1997) whose relative proximity to Spy raises the possibility of a geographical component in the distribution of the morphological variants of the deltoid tuberosity.

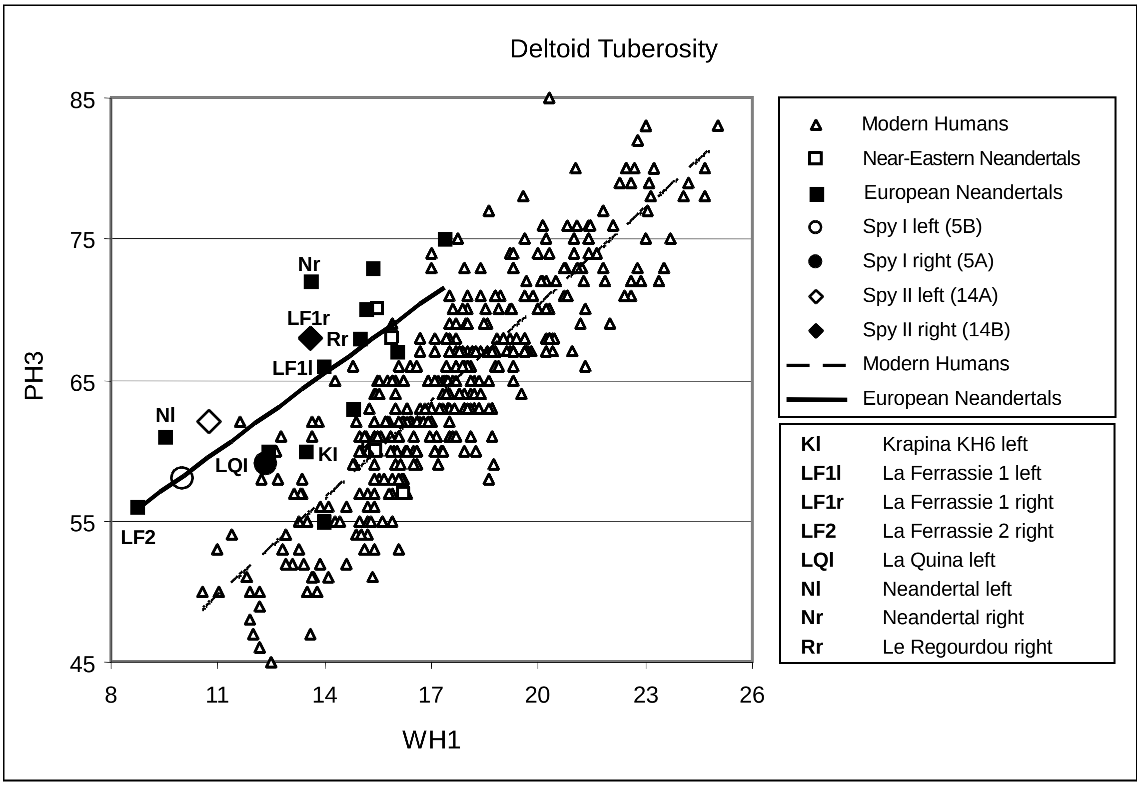

Figure 4. Bivariate analysis of the deltoid tuberosity comparing the tuberosity width (WH1) measured at the 5/12 of the bone maximum length level, and the shaft perimeter (PH3) measured at the same level. The European Neandertals and modern human sample regression lines are represented.

FUNCTIONAL ANATOMY

Upper limb asymmetry

The asymmetry pattern of the upper limb bones suggests a right handedness for both Spy I and Spy II. If our attribution of both Spy 6 and Spy 15B radii to Spy II is correct, there is a particularly marked asymmetry in the interosseus borders. The Spy 6 (left) border is the longest while the Spy 15B (right) border is the most developed. A left dominance of the length of the interosseus border in a supposedly right handed individual is commonly found in modern humans as well (personal data). Only the Neandertal radii of Regourdou 1 are complete enough to calculate the interosseus border length asymmetry. The value (106.1) matches the modern humans average. On the contrary, the value of 161.6 roughly estimated for Spy (see * on Table 6 and SF1) would be unusually high considering the fact that the maximum asymmetry index observed in the modern sample is 136.3. Given the still debated role of the interosseus border (see below), such a strong dissymmetry in Spy II is currently difficult to interpret.

The asymmetry of the humeral shaft (Figure 5A) is particularly interesting to consider since it shows curves that are parallel between Spy II and the male Neandertals on the one hand, and between Spy I and the Tabun C1 female on the other hand. Although this observation is of functional rather than morphological nature, this would be consistent with the hypothesis of a sexual dimorphism in Spy. In Figure 5A, the male Neandertals and Spy II also show a greater humeral shaft asymmetry than the Tabun C1 female and Spy I. This could indicate a strong sex-related division of labor in Spy, and in Neandertals in general (see also Ben-Itzhak *et al.*, 1988). In any case, and regardless of their sex, the dissimilarity in the levels of asymmetry existing between Spy I and Spy II suggests very different patterns of physical activity, with more lateralised and more specialised occupations in Spy II.

Both Spy individuals, moreover, show particularly asymmetrical deltoid tuberosities. If Spy I is indeed a female, this high level of asymmetry would be close to that observed in Tabun C1. In contrast, if Spy II is a male, his asymmetry is greater than in the other currently known male Neandertals. In this case, the nature of his particular pattern of deltoid muscle activity remains an open question.

The high level of cortical asymmetry of the Spy II humeri has caught the attention of Trinkaus *et al.* (1994). It is indeed comparable to the La Quina 5 asymmetry percentage which has been considered as potentially pathological by Martin (1923) and Trinkaus *et al.* (1994) precisely because of its very high value, even though there is no trace of pathology on the preserved parts of the upper limb. Figure 5B shows that, except for the already cited particularly asymmetrical deltoid tuberosity width (WH1), the values of external shaft asymmetry of Spy II usually fall below the range of variation of the non-pathological Neandertals. So, contrary to the pathological (Neandertal 1) or reputedly so (La Quina 5) Neandertals who show both high asymmetries of the cortical and external dimensions of the humeri, Spy II only displays a noticeable cortical lateralisation. Although the hypothesis of a trauma on the upper limb cannot be excluded given some puzzling features (such as an unusually large radial tuberosity, a particularly slender radial neck and a possibly strong interosseus border asymmetry), there is no obvious sign of pathology on what is left of the arm and forearm bones of the Spy Neandertals.

	Interosseus border asymmetry			
	n	*min*	*m ± s*	*max*
Modern Humans	97	100.0	106.1 ± 6.5	136.3
Regourdou 1			106.1	
Spy 6/Spy 15B			161.6*	

Table 6. Absolute asymmetry of the interosseus border lengths (maximum side / minimum side X 100). The interosseus border length is measured from the proximal extremity. * indicates that the Spy 15B state of preservation made it necessary to measure the border alone in both Spy 6 and 15B (see SF1). The result obtained for Spy must therefore be considered as a rough estimation.

The shoulder

The Spy I and Spy II humerus deltoid tuberosities are moderately developed and very narrow, even by Neandertal standards. According to Heim (1982) the Spy deltoid muscle insertion is so faint that it is difficult to observe. These features suggest a rather weakly developed muscle (Endo, 1971), and thus a reduced abduction strength in Neandertals including in Spy. The deltoid muscle is indeed the main arm abductor in modern humans. It is composed of three distinct sets of fibres. The anterior fibres flex and medially rotate the arm, the middle fibres abduct it and the posterior ones extend and laterally rotate the upper limb. A more detailed analysis of the Spy deltoid tuberosities however reveals a skewness, the anterior crest being longer and more developed than the lateral one (Figure 1a). Despite a weakly developed deltoid muscle, this could indicate a powerful role of the anterior part of the deltoid muscle as a flexor and, to a lesser extent, as an internal rotator. The adduction, internal rotation and flexion movements are also ensured by the pectoralis major. The insertion of this muscle is clearly visible on Spy I left (5B), and it is preserved in its most distal part on both Spy II humeri. These insertion sites form very developed, raised and smooth ridges that suggest powerful muscles. The same description is in accordance with the insertion for the teres major whose distal part is present on the Spy I left humerus. This muscle is involved in external rotation and extension. As a whole, the remaining clues of the shoulder physiology of the Spy Neandertals therefore suggest a reduced abduction strength but powerful flexion/extension and rotation movements.

The elbow

The Spy II elbow morphology (SF16) suggests powerful flexion and extension movements.

The trochlear notch of the ulna is very anteriorly oriented with a weakly projected coronoid process. As a consequence, the contact between the coronoid process and the humeral septum is delayed allowing complete flexion movements. The pin size holes and translucent area in the olecranon fossae moreover indicate a thin humeral septum which seems to be linked, when totally perforated, to ample flexion/extension potential in modern humans (Manouvrier, 1921; Glanville, 1967; Mays, 2008). Despite the deep and vast olecranon fossa, articulation of the humeri and ulnae however shows a reduced extension movement.

The insertions of the primary and secondary muscles responsible for the flexion and extension movements have been described as well-developed and/or located in mechanically advantageous positions in Neandertals (Aiello & Dean, 1990; Hambücken, 1993a, 1998; Holliday *et al.*, 1993; Churchill, 1994). This is also true for the Spy fossils.

The briefness of the coronoid process and weak prominence of the brachialis insertion of the Neandertals, including Spy II, must however have weakened the elbow in extension (Hambücken, 1998; SF17) since this area plays a role as a bracket in the modern human ulnae (Kapandji, 1973; Sénégas *et al.*, 1980). This hypothesis is in line with the study of Trinkaus & Churchill (1988) which concluded from the trochlear notch morphology that the elbow was more resistant in partial flexion in Neandertals and in extension in modern humans.

According to Trinkaus & Churchill (1988), the medial orientation of the radial tuberosity of most Neandertals suggests a powerful supination by maintaining the force moment during the entire movement while it disappears sooner when the orientation is more anterior (see also Aiello & Dean, 1990). This is also true in Spy 6, although the orientation of its radial tuberosity is not totally medial. It is noteworthy to point out that the supinator role of the biceps brachialis is maximal when the forearm is partially flexed. This would be consistent with the hypothesis of Trinkaus & Churchill (1988) that the Neandertal elbow was commonly used and more resistant in partial flexion (see also Hambücken, 1998).

The pronator teres insertions of the Neandertals have been described as well-developed by Heim (1982) and Trinkaus (1983). Moreover, these insertions are placed on the radial shaft bending which is accentuated in

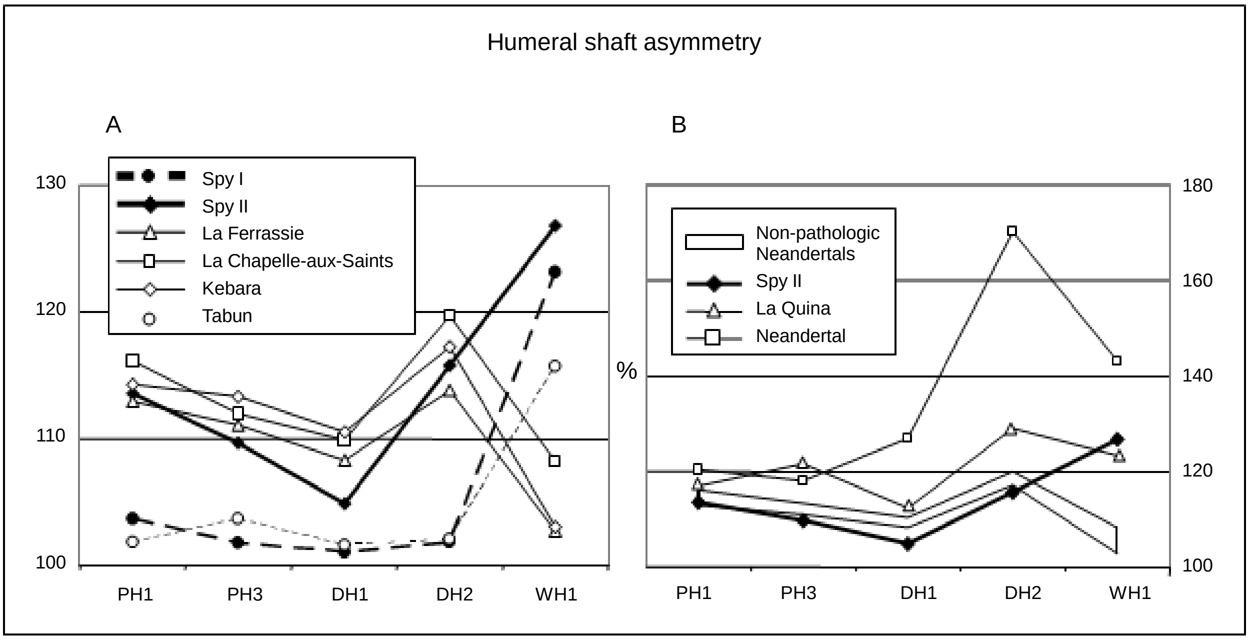

Figure 5. Absolute asymmetry degree of the humeral shafts of the Neandertals (maximum side / minimum side X 100).
A: Comparison between Spy I, Spy II and the currently known sexed Neandertals as identified by Berger & Trinkaus (1995); B: Comparison of Spy II to the non-pathological Neandertals (La Chapelle-aux-Saints 1, Kebara 2 and La Ferrassie 1) and to the pathological La Quina 5 and Neandertal 1 individuals.
Dimensions abbreviations as in Figure 3.

Neandertals (Trinkaus & Churchill, 1988; Aiello & Dean, 1990; Hambücken 1993a). This would indicate a powerful pronation in Neandertals, including in the case of Spy II.

The pronation limiting factor is, however, the diaphyses contact during the radius and ulna crossing. Neandertals, including the Spy fossils, display an array of features that could have moved the shafts apart, and therefore delayed their contact (Hambücken, 1998; SF17). The radius bending and the proximal ulna projection are indeed marked, whereas the insertion for the brachialis muscle of the ulna is only moderately prominent. The proximally placed maximum convexity of the humerus capitulum suggests a high position of the flexed radius in comparison with the ulna (see also Heim, 1974). The very homogeneous height of the articular periphery of the Spy 6 radius would indicate an extended radius rotation. The oblique orientation and significant height of the Spy radial notch could have retained the radio-ulnar contact when the diaphysis axis bends over during an extended rotation.

The shallowness of the Spy humeral trochlear gorges would have promoted slight medio-lateral ulna movements (Hambücken, 1998) by limiting the joint congruence. These movements, amplified by the bone length, are required to maintain the manual precision during the forearm rotation (Kapandji, 1973; Williams & Warwick, 1980).

The briefness of the interosseus border of the Spy radii, and their possibly very asymmetrical lengths (see above), are more difficult to interpret. The lateral pillar of the humeral pallet, situated above the radius, is wider than the medial one, and it has a “force bearing” role (Le Floch, 1978, 1982). Together with the very narrow medial pillar of the Neandertals, the shortness of the interosseus border of their radii could indicate a limited force transfer between the radius and ulna when the elbow is in extension (Hambücken, 1998). One of the interosseus membrane roles is indeed to convey, via the ulna, the forces sustained through the hand by the radius (Halls & Travill, 1964; Schneiderman *et al.*, 1993). This limited force transfer could have partially compensated the weakness of the Neandertal coronoid process (Hambücken, 1998; SF17).

ACKNOWLEDGEMENTS

I wish to warmly thank Patrick Semal, Bruno Maureille and Hélène Rougier for inviting me to participate to this study. I am particularly grateful to Patrick Semal for providing the pictures and for processing the bone cross-sections. I also wish to thank all the persons who welcomed me in their institution during the study of the fossils and modern human bones, as well as Bruno Bontempi and Thomas Durkin for English revision.

BIBLIOGRAPHY

AIELLO L. & DEAN C., 1990. *An introduction to human evolutionary anatomy*. New York, Academic Press: 569 p.

BEN-ITZHAK S., SMITH P. & BLOOM R. A., 1988. Radiographic study of the humerus in Neandertals and *Homo sapiens sapiens*. *American Journal of Physical Anthropology*, **77** (2): 231-242.

BERGER T. D. & TRINKAUS E., 1995. Patterns of trauma among the Neandertals. *Journal of Archaeological Sciences*, **22** (6): 841-852.

BOULE M., 1911. L'homme fossile de La Chapelle-aux-Saints. *Annales de Paléontologie*, **6**: 111-172.

BOULE M., 1912. L'homme fossile de La Chapelle-aux-Saints. *Annales de Paléontologie*, **7**: 85-192.

BOULE M., 1913. L'homme fossile de La Chapelle-aux-Saints. *Annales de Paléontologie*, **8**: 1-70.

CARRETERO J. M., ARSUAGA J. L. & LORENZO C., 1997. Clavicles, scapulae and humeri from the Sima de los Huesos site (Sierra de Atapuerca, Spain). *Journal of Human Evolution*, **33** (2-3): 357-408.

CHURCHILL S. E., 1994. *Human upper body evolution in the Eurasian Later Pleistocene*. Ph.D. Dissertation, University of New Mexico, Albuquerque: 395 p.

CHURCHILL S. E. & SMITH F. H., 2000. A modern human humerus from the early Aurignacian of Vogelherdhöhle (Stetten, Germany). *American Journal of Physical Anthropology*, **112** (2): 251-273.

DE LUMLEY M.-A., 1973. *Anténéandertaliens et Néandertaliens du bassin méditerranéen occidental européen*. Études du Quaternaire, mémoire n°2, Université de Provence: 626 p.

ENDO B., 1971. Some characteristics of the deltoid tuberosity of the humerus in the West Asian and the European “classic” Neanderthals. *Journal of the Anthropological Society of Nippon*, **79**: 249-258.

ENDO B. & KIMURA T., 1970. Postcranial skeleton of the Amud man. *In*: H. SUZUKI & F. TAKAI (ed.), *The Amud man and his cave site*. Tokyo, The University of Tokyo: 231-406.

FRAIPONT J. & LOHEST M., 1887. La race humaine de Néanderthal ou de Canstadt en Belgique. Recherches ethnologiques sur des ossements humains, découverts dans des dépôts quaternaires d'une grotte à Spy et détermination de leur âge géologique. *Archives de Biologie*, **7**/1886: 587-757.

GLANVILLE E. V., 1967. Perforation of the coronoid-olecranon septum. Humero-ulnar relationships in the Netherlands and African populations. *American Journal of Physical Anthropology*, **26** (1): 85-92.

HALLS A. A. & TRAVILL A., 1964. Transmission of pressure across the elbow joint. *The Anatomical Record*, **150**: 243-248.

HAMBÜCKEN A., 1993a. *Variabilité morphologique et métrique de l’humérus, du radius et de l’ulna des Néandertaliens. Comparaison avec l’Homme moderne.* Thèse de doctorat, Université Bordeaux I, Talence: 301 p.

HAMBÜCKEN A., 1993b. Révision des particularités de l’humérus des Néandertaliens européens. *Comptes Rendus de l'Académie des Sciences, Série III, Sciences de la vie*, **317**: 109-114.

HAMBÜCKEN A., 1997. La variabilité géographique des néandertaliens: apport de l'étude du membre supérieur. *Anthropologie et Préhistoire*, **108**: 109-120.

HAMBÜCKEN A., 1998. Morphologie et fonction du coude et de l’avant-bras des Néandertaliens. *Bulletins et Mémoires de la Société d’Anthropologie de Paris*, n.s., **10** (3-4): 213-236.

HEIM J.-L., 1974. Les Hommes fossiles de la Ferrassie (Dordogne) et le problème de la définition des Néandertaliens classiques. *L'Anthropologie* (Paris), **78**: 81-112.

HEIM J.-L., 1982. *Les hommes fossiles de la Ferrassie. II. Les squelettes adultes (squelette des membres)*. Archives de l'Institut de paléontologie humaine, **38**: 272 p.

HOLLIDAY T. W., CHURCHILL S. E. & TRINKAUS E., 1993. *Modern human origins in Africa: the postcranial evidence*. Paper presented at the 1993 Annual Meeting of the American Association for the Advancement of Science.

KAPANDJI I. A., 1973. *Physiologie articulaire. Schémas commentés de la mécanique humaine. Fascicule I, membre supérieur*. Paris, Librairie Maloine, 4ème édition: 208 p.

KLEPPS S., AUERBACH J., CALHON O., LIN J., CLEEMAN E. & FLATOW E., 2004. A cadaveric study on the anatomy of the deltoid insertion and its relationship to the deltopectoral approach to the proximal humerus. *Journal of Shoulder and Elbow Surgery*, **13** (3): 322-327.

LE FLOCH P., 1978. Les piliers de la palette humérale. *Mémoire du Laboratoire d'Anatomie de la Faculté de Médecine de Paris*, **35**: 1-175.

LE FLOCH P., 1982. The distal humerus: a structure with two pillars. *Anatomy Clinic*, **4**: 235-244.

MANOUVRIER L., 1921. *Sur l'interprétation anatomique de la perforation olécrânienne*. Rapport présenté au Congrès de l'Association française pour l'avancement des Sciences: 51 p.

MARTIN H., 1923. *Recherches sur l'évolution du Moustérien dans le gisement de La Quina (Charente). II: L'Homme fossile.* Paris, Octave Doin: 147 p.

MARTIN R., 1914. *Lehrbuch der Anthropologie.* Stuttgart, Jena Verlag von Gustav Fischer: 1181 p.

MARTIN R. & KNUSSMANN R., 1980. *Anthropologie. Handbuch der vergleichenden Biologie des Menschen, Band I: Wesen und Methoden der Anthropologie, Teil 1: Wissenschaftstheorie, Geschichte, morphologische Methoden*. Stuttgart, Gustav Fischer: 742 p.

MAYS S., 2008. Septal aperture of the humerus in a medieval human skeletal population. *American Journal of Physical Anthropology*, **136** (4): 432-440.

McCOWN T. D. & KEITH A., 1939. The Stone Age of Mount Carmel, Vol. 2: The fossil human remains from the Levalloiso-Mousterian. Oxford, Clarendon Press: 390 p., 28 pl. h.t.

MORANT G. M., 1927. Studies of Paleolithic man. II. A biometric study of Neanderthaloid skulls and their relationships to modern racial types. *Annals of Eugenics*, **2**: 318-381.

PATTE E., 1955. *Les Néanderthaliens. Anatomie, physiologie, comparaisons*. Paris, Masson & Cie: 559 p.

SCHNEIDERMAN G., MELDRIUM R. D., BLOEBAUM R. D., TARR R. & SARMIENTO A., 1993. The interosseus membrane of the forearm: structure and its role in Galeazzi fractures. *Journal of Trauma*, **35**: 879-885.

SEMAL P., ROUGIER H., CREVECOEUR I., JUNGELS C., FLAS D., HAUZEUR A., MAUREILLE B., GERMONPRÉ M., BOCHERENS H., PIRSON S., CAMMAERT L., DE CLERCK N., HAMBUCKEN A., HIGHAM T., TOUSSAINT M. & VAN DER PLICHT J., 2009. New Data on the Late Neandertals: Direct Dating of the Belgian Spy Fossils. *American Journal of Physical Anthropology*, **138** (4): 421-428.

SÉNÉGAS J., LAVIGNOLLE B. & VITAL J. M., 1980. *Anatomie fonctionnelle. I. Le membre supérieur.* Bordeaux, Édition Bergeret: 150 p.

SMITH F. H., 1976. *The Neandertal remains from Krapina: A descriptive and comparative study.* University of Tennessee, Department of Anthropology, Report of investigation, **15**: 359 p.

SMITH F. H., 1980. Sexual differences in European Neanderthal crania with special reference to the Krapina remains. *Journal of Human Evolution*, **9** (5): 359-375.

SOLLAS W. J., 1907. On the cranial and facial characters of the Neandertal race. *Philosophical transactions of the Royal Society of London, series B, Biological sciences*, **199**: 281-339.

THOMA A., 1975. Were the Spy fossils evolutionary intermediates between Classic Neandertal and Modern Man? *Journal of Human Evolution*, **4** (5): 387-410.

TRINKAUS E., 1980. Sexual differences in Neandertal limb bones. *Journal of Human Evolution*, **9** (6): 377-397.

TRINKAUS E., 1983. *The Shanidar Neandertals*. New York, Academic Press: 502 p.

TRINKAUS E. & CHURCHILL S. E., 1988. Neandertal Radial Tuberosity orientation. *American Journal of Physical Anthropology*, **75** (1): 15-21.

TRINKAUS E., CHURCHILL S. E. & RUFF C. B., 1994. Postcranial robusticity in *Homo.* II: humeral bilateral asymmetry and bone plasticity. *American Journal of Physical Anthropology*, **93** (1): 1-34.

VANDERMEERSCH B., 1981. *Les Hommes fossiles de Qafzeh (Israël)*. Cahiers de Paléoanthropologie. Paris, CNRS Éditions: 319 p.

VANDERMEERSCH B., 1991. La ceinture scapulaire et les membres supérieurs. *In*: O. BAR-YOSEF & B. VANDERMEERSCH (ed.), *Le squelette mous-*

térien de Kébara 2. Cahiers de Paléo-anthropologie. Paris, CNRS Éditions: 157-178.

VANDERMEERSCH B. & TRINKAUS E., 1995. The postcranial remains of the Regourdou 1 Neandertal: the shoulder and arm remains. *Journal of Human Evolution*, **28** (4): 439-476.

WILLIAMS P. L. & WARWICK R., 1980. *Gray's anatomy.* 36th British Edition, W. B. Philadelphia, Saunders Company: 1578 p.

AUTHOR'S AFFILIATION

Anne HAMBÜCKEN
Earth and History of Life
Royal Belgian Institute of Natural Sciences
29, Vautier Street
1000 Brussels
Belgium
anne.hambucken@free.fr